International Journal of Research in Engineering and Innovation (IJREI)
journal home page: http://www.ijrei.com
ISSN (Online): 2456-6934

ORIGINAL ARTICLE

Optimization of FSW parameters on mechanical properties of AA6082 and AA7475 by response surface methodology

Prem Kumar[1], Kalyan Singh[1], Azazullah[2]

[1]*Department of Mechanical Engineering College, Delhi Technological University, Delhi, India*
[2]*Department of Science Technology & Technical Education, Government Polytechnic West Champaran, Bettiah*

Article Information

Received: 17 September 2023
Revised: 28 December 2023
Accepted: 3 January 2023
Available online: 8 January 2024

Keywords:

Friction stir welding
Microhardness
Tensile strength
Response surface methodology
ANOVA

Abstract

This research endeavors to formulate a mathematical model using Response Surface Methodology (RSM) to forecast hardness, Ultimate Tensile Strength (UTS), and percentage elongation of friction stir welded (FSW) joints between AA6082 and AA7475 alloys. The experimental design incorporated three factors at three varying levels, culminating in 20 distinct experimental runs. The model's validity was assessed through an analysis of variance at a 95% confidence interval, focusing on three input parameters: Tool Tilt Angle (TTA), Tool Rotational Speed (TRS), and Welding Speed (WS), against output responses including hardness, UTS, and percentage strain. The study identified TRS and WS as pivotal parameters influencing the mechanical attributes of the weldments. Optimal UTS (225.07 MPa) and strain percentage (19.35) were attained at specific TRS, WS, and TTA settings, whereas suboptimal results were observed under different conditions. Further analysis revealed that plastic deformation, induced by tool stirring and elevated temperatures, facilitated Dynamic Recrystallization (DRX) of grains, resulting in a refined grain structure. Notably, the presence of sub-grains significantly bolstered the UTS of FSW joints, acting as barriers to dislocation movement and augmenting material strength and resilience. This refined grain structure observed in the FSW zones can be attributed to the combined effects of temperature, DRX, and plastic deformation at elevated rotational tool speeds.

1. Introduction

Friction stir welding (FSW) is a solid-state joining process of similar and dissimilar light metal alloys, offering distinct advantages over traditional fusion welding methods. Wayne M. Thomas and the TWI team patented and pioneered this method in 1991, with its formal recognition in 1993 [1]. One of the primary challenges with aluminum alloys, like the 2xxx and 6xxx series popular in aerospace and automotive applications, is their susceptibility to coarse microstructures and defects such as porosity during fusion welding. Such defects can substantially degrade the tensile properties of weldments [2, 3]. The innovation of FSW lies in its use of frictional heat and plastic deformation, eliminating the complications related to re-solidification and melting. Consequently, FSW facilitates the creation of high-quality, defect-free joints with superior mechanical properties [4]. The FSW tool's pivotal role is generating frictional heat and guiding material flow. This dual functionality enables the creation of robust joints between disparate metals or alloys, underscoring FSW's potential for joining dissimilar materials [5, 6]. The tangible benefits of FSW are manifold. Compared

Corresponding author: Prem Kumar
Email Address: prem181292@gmail.com
https://doi.org/10.36037/IJREI.2024.8105

to fusion welding, FSW offers reduced heat-affected zones, metals, resulting in minimized distortions and optimized joint efficiency [7]. This has catalyzed its adoption across critical industries like automotive, aerospace, and shipbuilding, where the method's defect-free outcomes and improved mechanical properties are highly prized [8]. Despite these merits, the welding parameters in FSW, such as tool rotational speeds (TRS) and welding speeds (WS), require meticulous optimization. For instance, studies on AA6082 and AA2014 alloys highlighted the significance of TRS variations, revealing the formation of large softened zones at higher TRS values [9]. Similarly, investigations into the FSW of AA7075 and AA6082 emphasized the criticality of parameters like TRS, WS, and tool pin profiles in determining joint quality [10]. Such insights underscored the importance of parameter combinations in achieving desired tensile strengths and mitigating defects like the coarsening of Mg2Si sediments [11]. Moreover, applying high heat input can introduce complexities in the metallurgical properties of FSW joints. However, with precise parameter optimization, the adverse effects on the ultimate tensile strength (UTS) and hardness can be alleviated [12-14]. Advancements in FSW are not limited to parameter optimization alone; they encompass integrating cutting-edge techniques like numerical simulations, machine learning, and artificial intelligence. Such integrations amplify the precision and efficiency of FSW parameter optimization by decoding intricate parameter interactions and predicting optimal combinations [15, 16]. Within this context, RSM emerges as a potent tool for mathematical modeling, capturing the nuanced relationships between variables and outcomes. enhanced welding speed, and versatility in joining varied Unlike methodologies with inherent limitations, such as the Taguchi method's constrained array fractions, RSM accommodates multiple parameters, enabling a holistic understanding of complex interactions [17-20]. Leveraging this, our research endeavors to construct a predictive mathematical model using RSM for the FSW joints of AA6082 and AA2014. Employing the Design Expert software, we conducted regression analyses, scrutinized response surface contour plots, and validated our model's robustness through ANOVA. Ultimately, this study aspires to furnish invaluable insights, paving the way for optimizing FSW parameters and elevating the quality and efficacy of welded joints in critical applications [21].

2. Material and Methods

The experimental configuration for crafting dissimilar AA6082 and AA7050 FSW joints utilized a numerical control FSW machine equipped with a rotating spindle, automated table, tool head, and welding fixture. The foundational materials were two AA7475 and AA6082 plates, each measuring 150 × 50 × 6.35 mm. Their chemical compositions include various elements, predominantly aluminum, ensuring their selection due to compositional similarities, industrial significance, distinct properties, and the potential to join dissimilar materials. Such attributes position AA6082 and AA7475 alloys as prime candidates for assessing the FSW process and elucidating its implications [21].

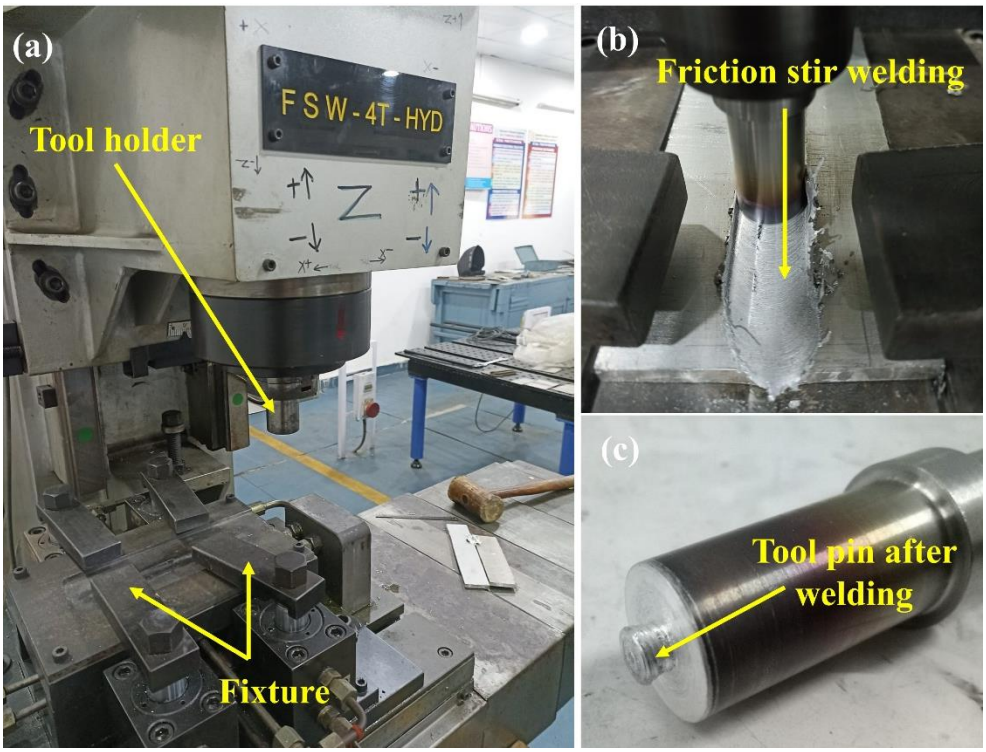

Figure 1: Experimental process of friction stir welding

The parameters for this study, detailed in Table 1, were derived from preliminary trials and aligned with the FSW machine's capabilities. Designing the experiment involved utilizing the Response Surface Methodology (RSM), focusing on three pivotal parameters: TRS, WS, and TTA, each with three distinct levels. Throughout the experiment, the H13 tool steel, characterized by a square pin profile. The experimental process is shown in Fig. 1. This choice was influenced by the square pin profile's aggressive stirring capabilities, generating superior shear forces and facilitating optimal material mixing [21]. The square pin's enhanced stirring action fosters improved metallurgical bonding and augments heat generation and dissipation during the FSW process. The design promotes efficient heat transfer, which is crucial for maintaining the requisite temperature range for seamless welding. Further, the strategic placement of the materials—AA6082 on the advancing side (AS) and AA7475 on the retreating side (RS)—follows recommendations from prior studies [22-25].

Table 1: Friction stir welding parameters range and its level

Parameters	Range	Levels		
		-1	0	1
A-TRS (rev/min)	500-800	500	650	800
B-WS (mm-min^{-1})	80-110	80	95	110
C-TTA (°)	0-2	0	1	2

Post-welding procedures involved allowing specimens to cool to room temperature. Subsequent tensile testing specimens were precisely sectioned using an EDM machine, adhering to ASTM E8 standard. For microstructure evaluations, samples were extracted from welded regions, meticulously polished through graded sandpapers (220 to 3000) and etched with Keller's reagent for approximately 8-10 seconds. These prepared specimens underwent thorough analysis using optical and scanning electron microscopy techniques.

3. Results and Discussion

3.1 Tensile strength

The Design Expert software orchestrated twenty experiments to discern the mechanical properties of FSWed joints of AA6082 and AA7475. Observations highlighted that Tool Rotational Speed (TRS) escalation corresponded with increased percent strain and Ultimate Tensile Strength (UTS). However, UTS and Welding Speed (WS) manifested an inverse relationship. Interestingly, optimal conditions at TRS 800 rev/min, WS 80 mm-min^{-1}, and TTA 2° approximated the UTS to that of the base material, emphasizing the necessity of a nuanced trade-off between UTS and hardness.

Elevated TRS levels fostered enhanced heat input, engendering ultrafine grain structures conducive to heightened UTS. Nonetheless, surpassing 800 rev/min ushered in excessive heat, culminating in micro-voids within the stir zone, potentially compromising structural integrity. UTS values fluctuated between 185 to 265 MPa across experiments, with the least UTS observed at specific parameters detailed in Fig.2. Temperature intricacies, grain coarsening, and cooling dynamics emerged as pivotal determinants modulating UTS. The propensity for cracking within the Heat-Affected Zone (HAZ) and Thermomechanically Affected Zone (TMAZ) underscores potential vulnerabilities, necessitating meticulous inspection and testing protocols [26, 27]. The study accentuates the imperative of judicious parameter modulation, rigorous inspections, and stringent quality assurance to ensure FSWed joint robustness. Conclusively, pinnacle UTS (260.25 MPa) and percent strain (16.36) were realized at TRS 800 rpm, WS 80 mm/min, and TTA 2°, encapsulating optimal conditions for FSWed joint performance.

3.2 Hardness measurement

The microhardness profile of FSWed joints in AA6082 and AA7475 is depicted in Fig. 4, showcasing variations influenced by several determinants. Factors encompass welding parameters, joint grain structure, and alloy composition, traditionally indicating higher microhardness in welded joints than in base materials [26, 27]. FSW induces pronounced plastic deformation and grain refinement, amplifying microhardness. Notably, research indicates microhardness values between 75 to 110 HV for these joints, contingent on specific FSW parameters. Elevated welding speeds and diminished tool rotational speeds generally yield augmented microhardness, predominantly attributed to intensified plastic deformation and grain refining effects.

While these observations provide overarching insights, exact microhardness metrics hinge on precise welding conditions, tool configurations, and additional variables. Consequently, referencing specialized research or engaging field experts is advised for comprehensive and accurate microhardness data on FSWed joints in AA6082 and AA7475.

Significantly, microhardness variations manifest across joint thicknesses, peaking in the stir zone (SZ)—where tool penetration occurs—and diminishing towards the Heat-Affected Zone (HAZ) and base metal. This zenith in SZ microhardness stems from the dissolution of precipitation phases and a refined recrystallized grain structure. The HAZ and TMAZ exhibit reduced hardness due to aging precipitates [28], coarser grain structures, and compromised heat dispersion. As depicted in Fig. 4, a peak hardness of 106.46 HV was evident at WS 95 mm-min^{-1}, TRS 800 rev/min, and TTA 1°, while the minimum at 77.43 HV, materialized at TRS 500 rev/min, WS 110 mm-min^{-1}, and TTA 0°.

3.3 Development of mathematical model

RSM amalgamates mathematical and statistical techniques to enhance process optimization and product quality. This methodology encompasses designing experiments to evaluate how various process parameters influence the desired outcome. Analyzing experimental outcomes via statistical models, RSM pinpoints the best parameter configurations for achieving the targeted response. Derived regression models from RSM elucidate current results and forecast outcomes for

novel parameter settings, thereby economizing time and resources by circumventing additional experiments. Moreover, tools like response surface and contour plots visually elucidate relationships between input and output variables [29], facilitating rapid and efficient identification of optimal process parameter configurations. The mathematical regression equation would be.

$$y = k_0 + k_1x_1 + k_2x_2 + k_3x_3 + k_{11}x_1^2 + k_{22}x_2^2 + k_{33}x_3^2 + k_{12}x_1x_2 + k_{13}x_1x_3 + k_{23}x_2x_3 \quad (1)$$

where y either of hardness, % strain, and UTS *while* x_1, x_2, and x_3 are TRS, WS, and TTA.

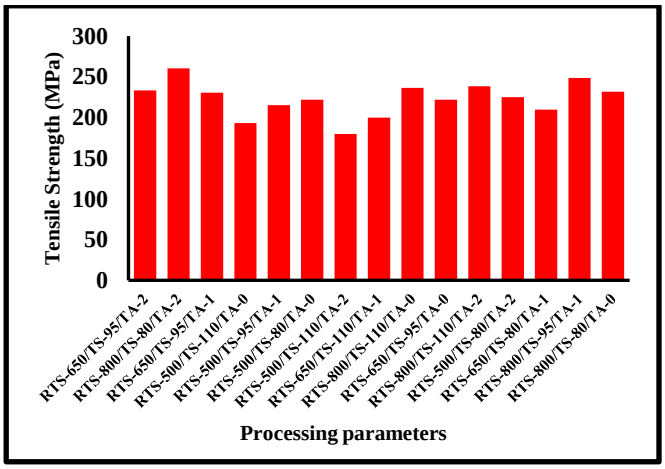

Figure 2: Variation of process parameters to the UTS.

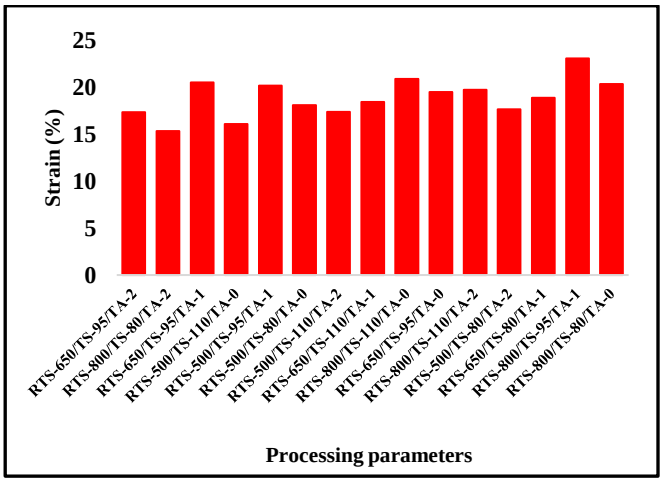

Figure 3: Variation of process parameters to the % strain

3.4 Adequacy of the developed model

The results gleaned from the Analysis of Variance (ANOVA) technique underscore the reliability and validity of the developed models regarding Ultimate Tensile Strength (UTS), percentage elongation (% elongation), and hardness values. This assertion is grounded in statistical evidence: the Contour plots serve as pivotal tools in the realm of calculated Fratio value for the formulated model falls below the standard Fratio value when considering a 95% confidence interval (CI). Moreover, the prob > F values associated with all three models are less than 0.05. Such values signify that the model holds significance and, critically, that any potential lack of fit (LOF) is negligible.

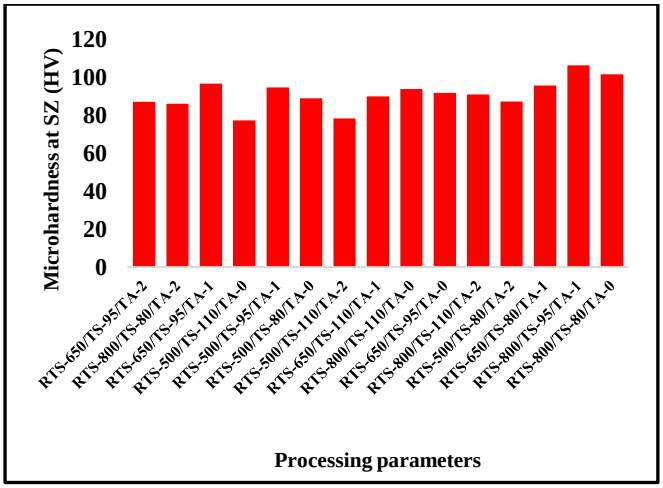

Figure 4: Microhardness variation to the input parameters at SZ

Additionally, inspecting the average percentage probability versus residual plots indicates a favorable normal distribution of residuals, aligning with desirable statistical assumptions. Furthermore, the juxtaposition of predicted versus experimental values underscores a robust alignment between the anticipated and actual responses [30, 31]. By subjecting all coefficients to rigorous scrutiny via the F-test within a 95% CI, refined models emerged for forecasting the microhardness, percentage strain, and UTS for friction stir-welded (FSWed) joints crafted from AA6082 and AA7475 alloys. The process of sculpting a mathematical model within the Response Surface Methodology (RSM) framework is multifaceted. It mandates meticulous experiment design, precise data collection, and adept model fitting. Employing such a methodological approach ensures that the resultant model captures the nuances of the process and stands as a reliable tool for optimization endeavors [32]. The intricate interplay between input variables and resulting outcomes is elegantly captured through empirical correlations articulated via equations, offering insights and avenues for process refinement and enhancement.

$$UTS = -158.69 + 0.7413A + 12.94B + 5.27C + 0.00313AB + 0.0342\ AC - 0.3586\ BC + 0.0004A^2 - 0.08B^2 + 4.84C^2$$

$$\%\ strain = 0.1995 - 0.105A + 1.06B + 2.29C + 0.0039AB - 0.00584\ AC + 0.0467\ BC + 0.00006A^2 - 0.007B^2 - 1.836C^2$$

$$Hardness = 33.06 - 0.232A + 2.8B + 10.81C + 0.00098AB - 0.014\ AC + 0.127\ BC + 0.000145A^2 - 0.0198B^2 - 7.87C^2$$

optimization, aiding in identifying optimal parameters and

attaining maximum output responses. By offering a graphical representation, these plots effectively juxtapose two critical parameters against each other while holding other variables constant. Such visualizations illuminate the relationship between the output response and specific process parameters. Consequently, engineers and researchers can discern the optimal values of these parameters that culminate in the most favorable outcomes.

Moreover, the utility of contour plots extends beyond mere visualization. Upon pinpointing a stationary point via these plots, it becomes imperative to delve deeper. Specifically, it's essential to analyze the response surface proximate to this point. This analysis elucidates whether the identified point is a peak (maximum), trough (minimum), or saddle point in the response context [33]. The ANOVA methodology is another critical evaluative tool. By subjecting the formulated model to the rigors of ANOVA, its adequacy and reliability come to the fore. Encouragingly, the outcomes of this analysis underscored the significance and efficacy of the model, mainly when evaluated within a 95% confidence interval.

Table 2: ANOVA table of tensile strength

Source	Sum of square	DOF	Mean square	F Value	P Value	
Model	6109.62	9	678.85	17.57	< 0.0001	significant
A-Tool Rotation Speed	3237.09	1	3237.09	83.76	< 0.0001	
B-Traverse Speed	1009.82	1	1009.82	26.13	0.0005	
C-Tilt angle	99.86	1	99.86	2.58	0.1390	
AB	398.75	1	398.75	10.32	0.0093	
AC	211.36	1	211.36	5.47	0.0414	
BC	231.55	1	231.55	5.99	0.0344	
A^2	230.49	1	230.49	5.96	0.0347	
B^2	901.93	1	901.93	23.34	0.0007	
C^2	64.55	1	64.55	1.67	0.2253	
Residual	386.47	10	38.65			
Lack of Fit	224.16	5	44.83	1.38	0.3659	not significant
Pure Error	162.32	5	32.46			
Cor Total	6496.10	19				

Table 3: ANOVA table of % strain

Source	Sum of square	DOF	Mean square	F Value	P Value	
Model	61.03	9	6.78	18.25	< 0.0001	significant
A-Tool Rotation Speed	10.06	1	10.06	27.08	0.0004	
B-Traverse Speed	0.4884	1	0.4884	1.31	0.2782	
C-Tilt angle	5.48	1	5.48	14.74	0.0033	
AB	6.46	1	6.46	17.40	0.0019	
AC	6.14	1	6.14	16.54	0.0023	
BC	3.93	1	3.93	10.59	0.0087	
A^2	5.15	1	5.15	13.87	0.0039	
B^2	7.05	1	7.05	18.99	0.0014	
C^2	9.27	1	9.27	24.97	0.0005	
Residual	3.71	10	0.3714			
Lack of Fit	1.78	5	0.3569	0.9244	0.5333	not significant
Pure Error	1.93	5	0.3860			
Cor Total	64.74	19				

Tables 2-4 present the outcomes of the Analysis of Variance (ANOVA) tests concerning the output solutions. A striking observation across these tables is the considerably significant Fisher's F value associated with each model, underscoring its robustness and appropriateness. For instance, the expanded UTS model boasts a notable Fisher's F value of 17.57, signifying a marked enhancement in significance. This F-value's magnitude, however, may occasionally be attributable to minimal noise, albeit with a mere 0.01 percent probability of error. Delving deeper into the specifics, the Fisher's F value for the Lack of Fit (LOF) stands at 0.1.38, subtly emphasizing that any discrepancies or gaps are negligible. It's imperative to contextualize these findings by assessing the residual error value delineated in Table 3, which is at 386.47. This sum amalgamates the intrinsic significance of pure error, quantified at 162.32, with the LOF's value pegged at 224.16. Similarly, when analyzing the percent strain model, a Fisher's F value of 57.91 emerges, corroborating the model's saliency and relevance, analogously, this F-value's interpretation suggests the potential for nominal noise interference, albeit with a minuscule 0.01 percent likelihood. Furthermore, the Fisher's F value for the LOF in this context stands at 0.3536, again pointing to its inconsequential nature. Collectively, these metrics and their interpretations reaffirm the appropriateness and credibility of the established models.

Table 4: ANOVA table of microhardness

Source	Sum of square	DOF	Mean square	F Value	P Value	
Model	952.53	9	105.84	21.02	< 0.0001	significant
A-Tool Rotation Speed	270.92	1	270.92	53.80	< 0.0001	
B-Traverse Speed	85.09	1	85.09	16.90	0.0021	
C-Tilt angle	57.46	1	57.46	11.41	0.0070	
AB	38.90	1	38.90	7.72	0.0195	
AC	38.81	1	38.81	7.71	0.0196	
BC	29.11	1	29.11	5.78	0.0370	
A^2	29.11	1	29.11	5.78	0.0370	
B^2	54.61	1	54.61	10.85	0.0081	
C^2	170.60	1	170.60	33.88	0.0002	
Residual	50.35	10	5.04			
Lack of Fit	13.45	5	2.69	0.3644	0.8539	not significant
Pure Error	36.91	5	7.38			
Cor Total	1002.89	19				

The Fisher's F value is a pivotal statistical metric to ascertain the significance of variance among different group means. Here, a notable Fisher's F value of 21.02 for the hardness model strongly indicates the model's validity. This value implies a mere 0.01% likelihood that the model's emergence is attributable to random fluctuations. Moreover, the Fisher's F value concerning the Lack of Fit (LOF) stands at 0.3644, underscoring its negligible influence on the model's overall suitability. The coefficient of determination (R^2) is pivotal to further gauge the model's efficacy. The R^2 values for UTS, % elongation, and hardness are impressively high at 0.9735, 0.9812, and 0.9797, respectively. In essence, this study elucidates crucial insights into the intricate interplay between response variables and their determinants within the realm of FSW. The RSM is a pivotal tool for optimizing input and output responses within the welding parameters of AA6082 and AA7475 materials. This method constructed a comprehensive model, facilitating the visualization of intricate relationships through 3D and contour plots delineating optimal parameters. These plots vividly depict the variations, with blue denoting low peak intensity and red signifying heightened peak intensity [34, 35]. One of the pivotal findings pertains to the influence of welding speed (WS) on Ultimate Tensile Strength (UTS) and hardness. As WS escalates, UTS and hardness initially exhibit an upward trajectory, reaching an apex. However, surpassing this threshold, a decline ensues due to alterations in the temperature field, subsequently compromising the integrity of the Friction Stir Welded (FSW) joints. This pattern is further exemplified as UTS augments with an increase in Tool Rotational Speed (TRS). Yet, an intricate relationship unfolds when Tool Tilt Angle (TTA) is factored in. As illustrated in Figs. 5-6, while UTS initially ascends with TTA, it subsequently descends, underscoring the nuanced interplay of these parameters.

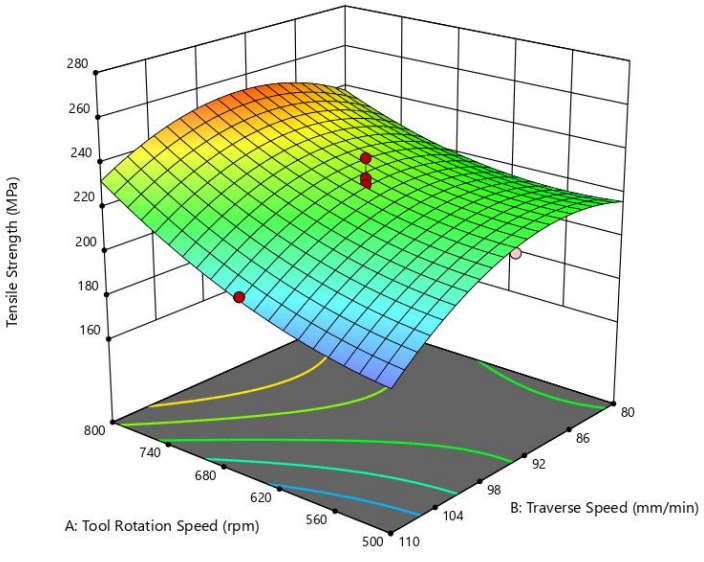

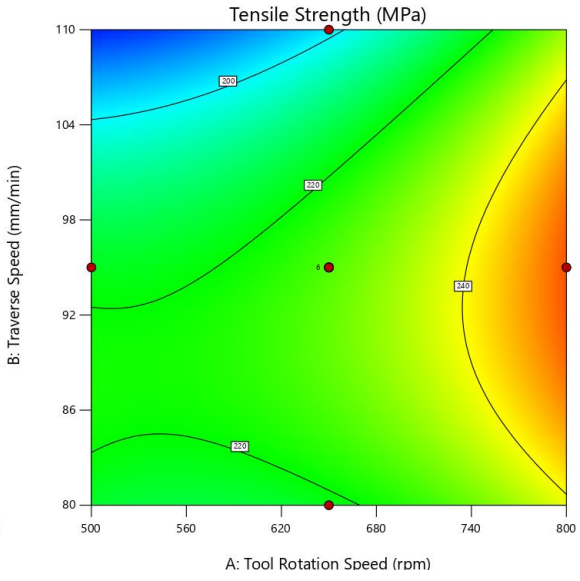

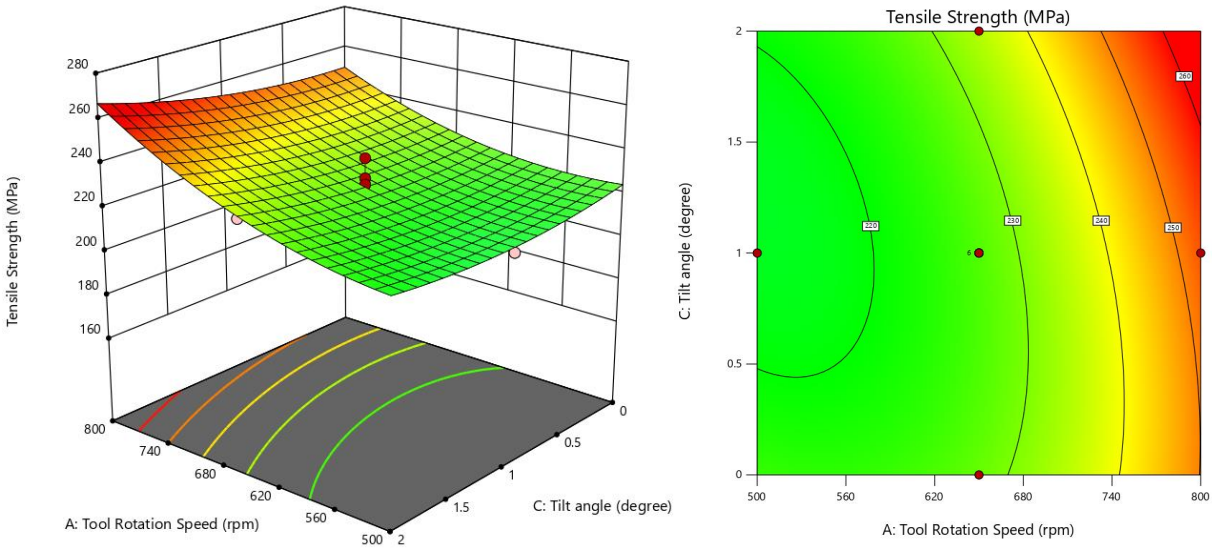

Figure 5: Surface plot and 3D contour for UTS

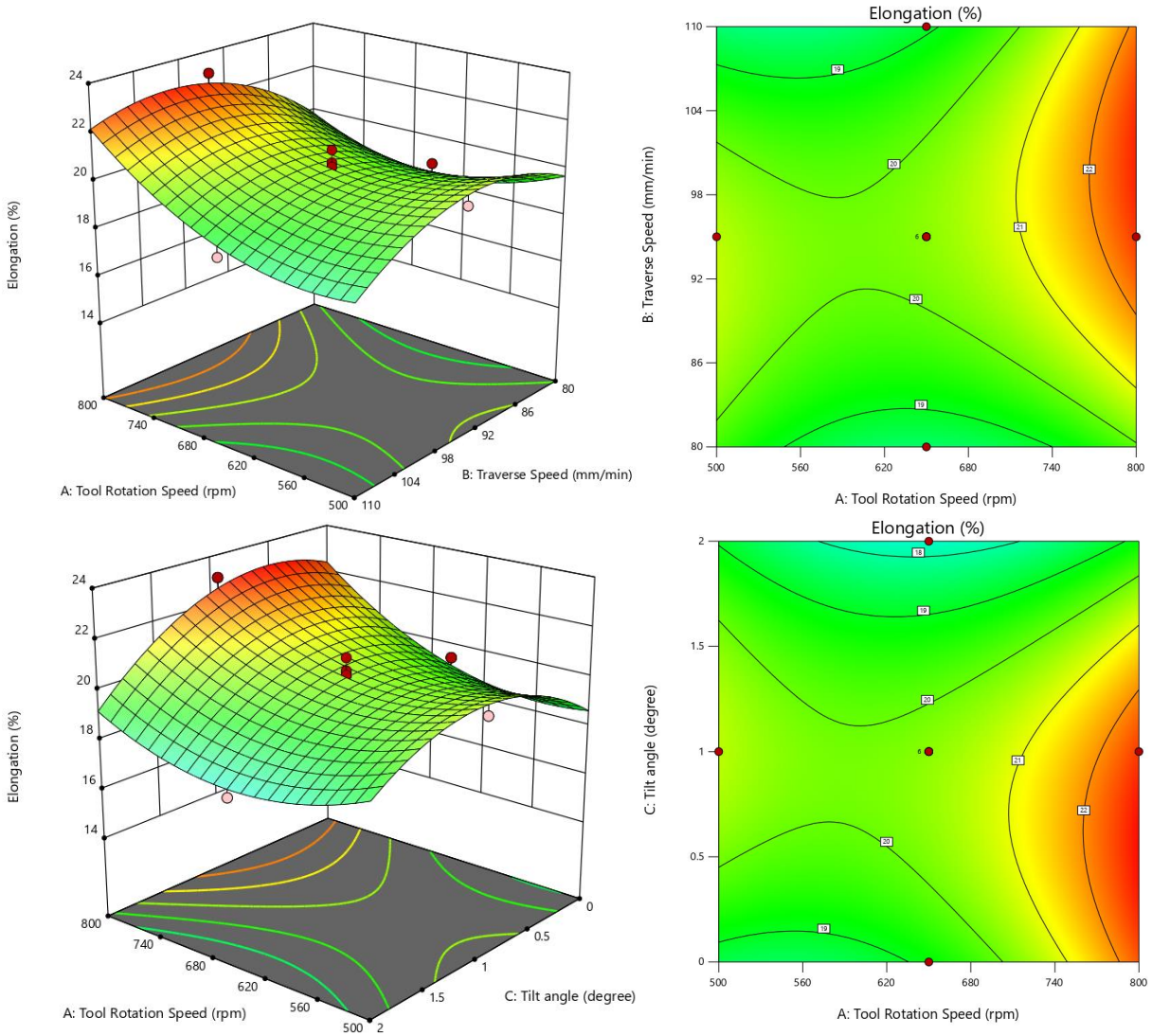

Figure 6: 3D contour and Surface response for % strain

Further analysis presented in Figs. 5, 6 elucidates the multifaceted variations in output responses relative to the input parameters. The observed trends reveal that UTS escalates proportionally with TRS increments. Contrarily, as both WS and TTA oscillate, UTS demonstrates a fluctuating pattern characterized by ascent and descent phases. The discernible increase in percent strain and hardness with escalating TRS is particularly noteworthy. However, as WS and TTA witness an increase, these metrics initially surge, only to diminish [36].

A pivotal aspect of this study is the assessment of the model's predictive prowess, elucidated in Fig. 7. Evidently, the model manifests commendable prediction capabilities, evidenced by the uniform dispersion between the projected and actual values. This consistent distribution and the scatter plot's alignment close to a 45° straight line proximate to actual values accentuate the model's efficacy. Such alignment underscores that the model's discrepancies are sporadic, fortifying its reliability. The robust correlation between the model's predicted outcomes and observations reaffirms its precision. This inherent capability of the model to discern and encapsulate intricate data patterns augments its utility. These findings underscore the model's proficiency in extrapolating accurate predictions, even when applied to novel, uncharted data scenarios.

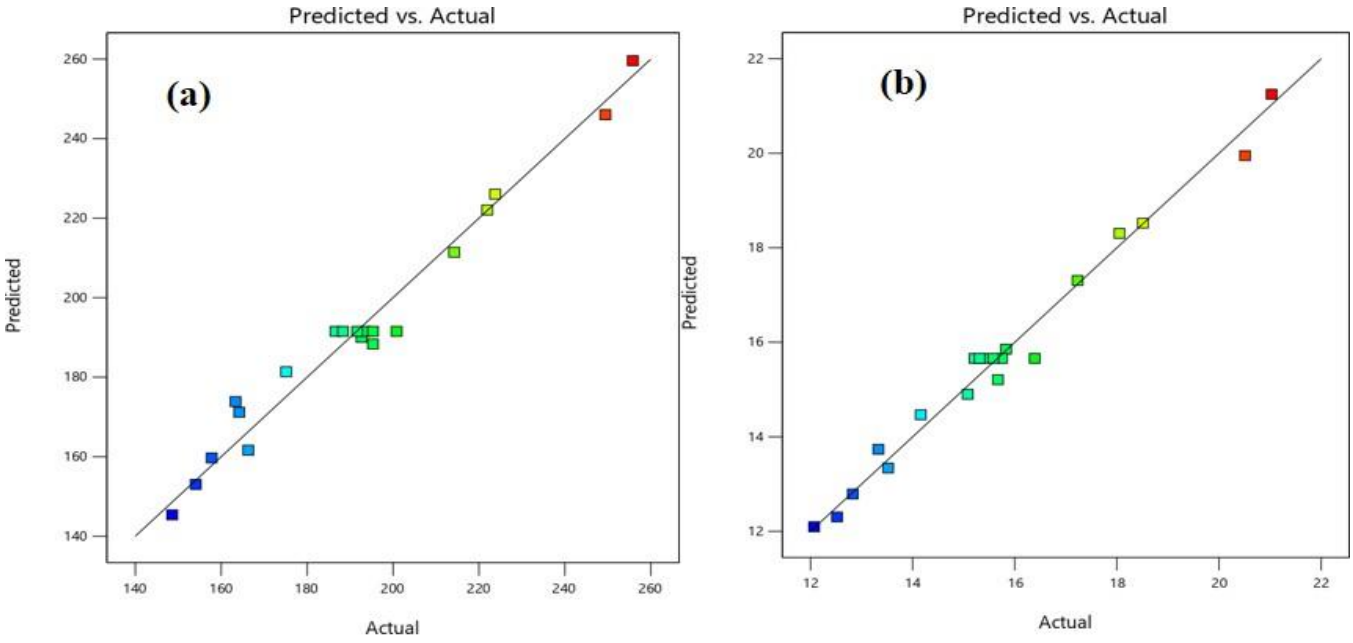

Figure 7: Actual and predicted scatter diagram, (a) UTS (b) % strain, (c) Microhardness

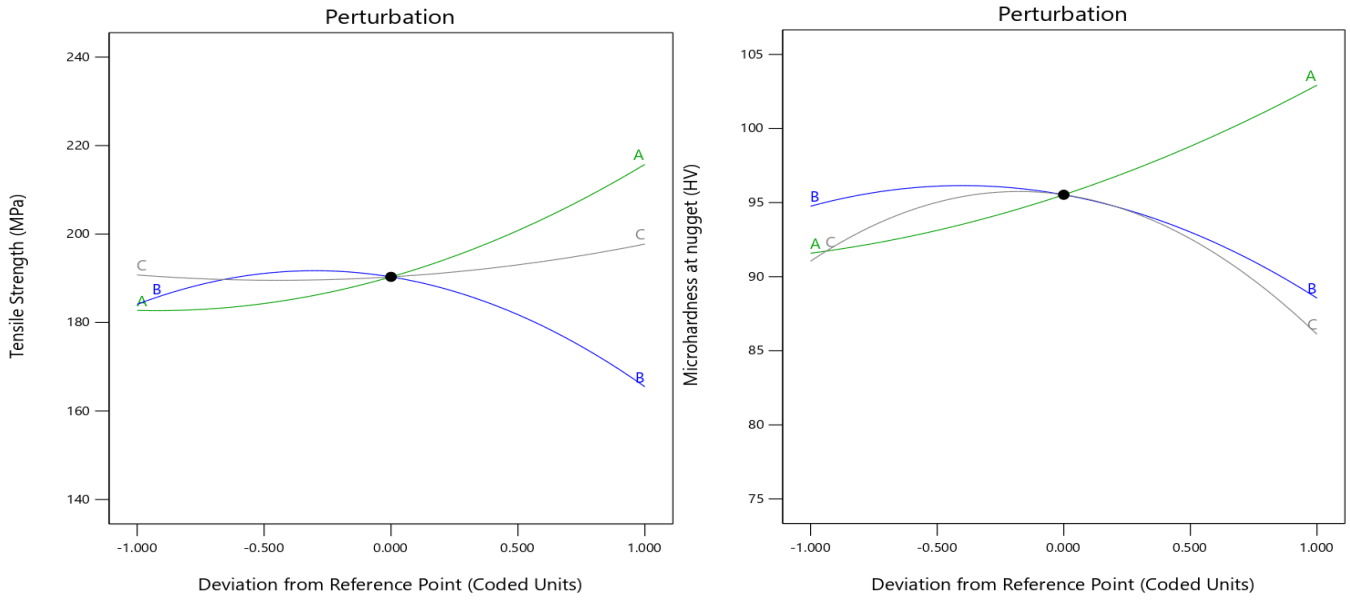

Figure 8: Perturbation curve, (a) UTS, (b) Microhardnes

The perturbation curve offers a visual insight into how variations in FSW parameters impact the mechanical attributes of the weld. This graphical representation delineates the relationship between each parameter's alteration and its effect on UTS, % strain, and hardness. Crucially, the curve's slope serves as a quantitative measure of sensitivity: a steeper slope signifies heightened sensitivity of the mechanical properties to alterations in the FSW parameters.

Fig. 8 shows that the TRS parameter boasts the most pronounced slope, underscoring its paramount importance. It indicates that manipulating the TRS holds considerable sway over augmenting the tensile strength of FSWed joints. Optimizing the TRS emerges as a pivotal strategy for bolstering the weld's mechanical prowess. The perturbation curve is an invaluable tool, elucidating the intricate interdependencies between FSW parameters and resultant mechanical attributes. Decoding this sensitivity paves the way for refined welding processes, ensuring the attainment of desired mechanical properties with precision.

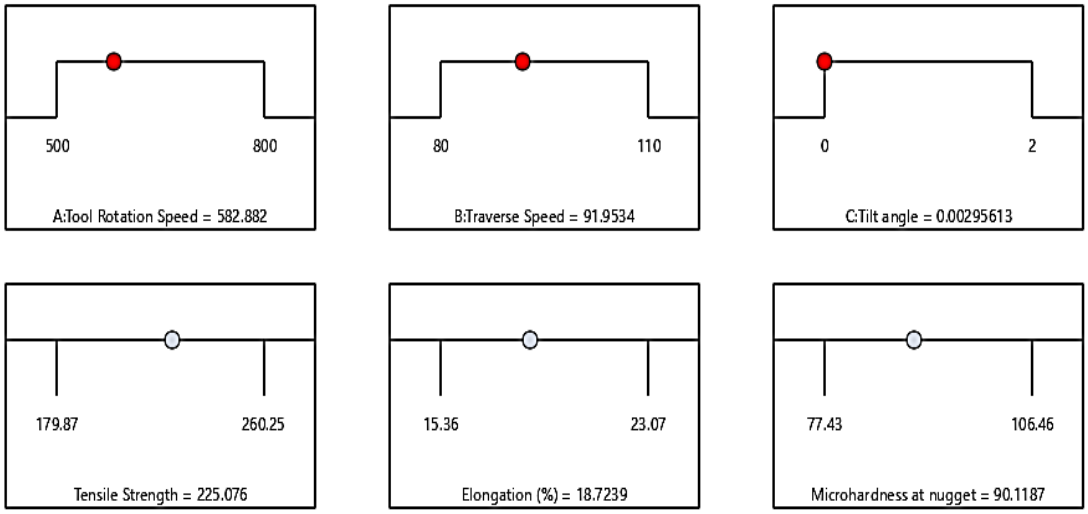

Figure 9: Optimize input and output responses of FSWed joint of AA6082 and AA7475

The multi-response optimization technique was harnessed to refine several objective functions within the FSW process concurrently. Specifically, the focal objective functions encompassed UTS, percent strain, and hardness within the SZ. Delving into the outcomes, the optimization endeavors achieved a UTS of 225.07 MPa, a percent strain of 15.40%, and a hardness reading of 90.11 HV within the SZ.

Furthermore, adjustments were made to the pivotal parameters TRS, WS, and TTA to attain these optimal mechanical attributes. Their refined values post-optimization stood at 582.88 rev/min, 91.95 mm-min^{-1}, and 0.002, respectively, as depicted in Fig. 9. These meticulously calibrated parameters spotlight the epitome of efficiency, ensuring that the FSW process is finely tuned to realize the envisaged mechanical properties within the SZ.

In essence, this multi-response optimization pinpointed the desired mechanical benchmarks and delineated the precise parameters—TRS, feed rate, and TTA—mandated to orchestrate an FSW process that consistently delivers these superior mechanical attributes.

4. Conclusions

The following conclusions were made from the present work.

- Base plates, each 6.2 mm thick and composed of AA6082 and AA7475 materials, were successfully manufactured using the FSW process. The study employed a CCD within the framework of RSM, focusing on three crucial input parameters: TRS, TS, and Tilt Angle.
- The highest recorded Ultimate Tensile Strength (UTS) achieved in the experiments was 260.25 MPa, occurring at a TRS of 800 rpm, a TS of 80 mm/min, and a TTA of 2°. Conversely, the lowest UTS value recorded was 179.87 MPa, observed at a TS of 110 mm/min, TRS of 500 rpm, and a TTA of 2°. The microhardness measurements indicated that the maximum value reached was 106.46 HV, obtained at a TS of 95 mm/min, TRS of 800 rpm, and a TTA 1°. In contrast, the minimum microhardness value of 77.43 HV was measured at a TS of 110 mm/min, TRS of 500 rpm, and a TTA of 0°.
- An empirical relationship was established between the input parameters and output responses, resulting in the determination of optimal values for UTS, % strain, and microhardness at the SZ. UTS, % strain, and microhardness at the SZ were optimized to 225.07 MPa, 18.72 %, and 90.11 HV, respectively, while TRS, feed rate, and TTA were tuned to 582.88 rpm 91.95 mm/min, and 0.003°, respectively
- When the TRS and TS increase, the grain size decreases in the SZ. Furthermore, when the TRS is high, the temperature in the SZ rises. No common flaws were observed at high TRS of welded joints of AA7475 and AA6082.

References

[1] Thomas, W.M., Nicholas, E.D., Needham, J.C., Murch, M.G., Templesmith, P., Dawes, C.J., 1991. Improvement relating to friction welding. Int. Patent Application No. PCT/GB92/02203, US Patent No. 5460317, EP Patent No. EP0653265A2.

[2] Sumit Jain, R.S Mishra, Husain Mehdi, Rajat Gupta, Amit Kumar Dubey, Optimization of processing variables of friction stir welded dissimilar composite joints of AA6061 and AA7075 using response surface methodology, Journal of Adhesion Science and Technology, 2023. https://doi.org/10.1080/01694243.2023.2243682.

[3] Jitendra Kumar, Gaurav Kumar, Husain Mehdi & Mukesh Kumar, Optimization of FSW parameters on mechanical properties of different aluminum alloys of AA6082 and AA7050 by response surface methodology. International Journal on Interactive Design and Manufacturing (2023). https://doi.org/10.1007/s12008-023-01425-2.

[4] Heidarzadeh, A., Khodaverdizadeh, H., Mahmoudi, A., Nazari, E., 2012. Tensile behavior of friction stir welded AA 6061-T4 aluminum alloy joints. Materials and Design 37, 166–173.

[5] Padmanaban, G., & Balasubramanian, V. Selection of FSW tool pin profile, shoulder diameter and material for joining AZ31B magnesium alloy – An experimental approach. Materials and Design 2009; 30(7): 2647–2656.

[6] Shaurya Bhatnagar, Gaurav Kumar, Husain Mehdi, Mukesh Kumar, Optimization of FSW parameters for enhancing dissimilar joint strength of AA7050 and AA6061 using Response Surface Methodology (RSM), 2023, https://doi.org/10.1016/j.matpr.2023.04.144.

[7] Lee WB, Yeon YM, Jung SB. The improvement of mechanical properties of friction-stir-welded A356 Al alloy. Mater Sci Eng 2003;A355:154-159.

[8] A.Nait Salah, Husain Mehdi, Arshad Mehmood, Abdul Wahab Hashmid, Chandrabhanu Malla, Ravi Kumar, Optimization of process parameters of friction stir welded joints of dissimilar aluminum alloys AA3003 and AA6061 by RSM, Materials Today: Proceedings, 56 (4), 1675-1684, 2021, https://doi.org/10.1016/j.matpr.2021.10.288

[9] Jonckheere, C., Meestera, B., Denquin, A., Simara. A., 2013. Torque, temperature and hardening precipitation evolution in dissimilar friction stir welds between 6061-T6 and 2014-T6 aluminum alloys. Journal of Materials Processing Technology 213,826–837.

[10] Abdul Wahab Hashmi, Husain Mehdi, Sipokazi Mabuwa, Velaphi Msomi & Prabhujit Mohapatra, Influence of FSP Parameters on Wear and Microstructural Characterization of Dissimilar TIG Welded Joints with Si-rich Filler Metal. Silicon, 14, 11131–11145, 2022. https://doi.org/10.1007/s12633-022-01848-8

[11] Abdellah Nait Salah, Sipokazi Mabuwa, Husain Mehdi, Velaphi Msomi, Mohammed Kaddami, Prabhujit Mohapatra, Effect of Multipass FSP on Si-rich TIG Welded Joint of Dissimilar Aluminum Alloys AA8011-H14 and AA5083-H321: EBSD and Microstructural Evolutions. Silicon, 14, 9925–9941, 2022.

[12] Raturi, M., Garg, A., Bhattacharya, A., 2019. Joint strength and failure studies of dissimilar AA6061-AA7075 friction stir welds: Effects of tool pin, process parameters and preheating. Engineering Failure Analysis 96, 570–588

[13] Heidarzadeh, A., Khodaverdizadeh, H., Mahmoudi, A., Nazari, E., 2012. Tensile behavior of friction stir welded AA 6061-T4 aluminum alloy joints. Materials and Design 37, 166–173.

[14] Husain Mehdi, Arshad Mehmood, Ajay Chinchkar, Abdul Wahab Hashmi, Chandrabhanu Malla, Prabhujit Mohapatra, Optimization of process parameters on the mechanical properties of AA6061/Al2O3 nanocomposites fabricated by multi-pass friction stir processing, materialstoday proceedings, 56(4), 2022, 1995-2003.

[15] Husain Mehdi, Lalit Batra, Abhendra Pratap Singh & Chandrabhanu Malla, Multi-response optimization of FSW process parameters of dissimilar aluminum alloys of AA2014 and AA6061 by response surface methodology (RSM). International Journal on Interactive Design and Manufacturing (2023). https://doi.org/10.1007/s12008-023-01409-2.

[16] Silva ACF, Braga DFO, de Figueiredo MAV et al (2015) Ultimate tensile strength optimization of diferent FSW aluminium alloy joints. Int J Adv Manuf Technol 79:805–814.

[17] Anil Kumar KS, Murigendrappa SM, Kumar H (2017) A bottom-up optimization approach for friction stir welding parameters of dissimilar AA2024-T351 and AA7075-T651 alloys. J of Materi Eng and Perform 26:3347–3367. https://doi.org/10.1007/ s11665-017-2746-z.

[18] Husain Mehdi, R.S. Mishra, An experimental analysis and optimization of process parameters of AA6061 and AA7075 welded joint by TIG+FSP welding using RSM, Advances in Materials and Processing Technologies, 8(1), 2022, 598-620.

[19] Meengam C, Sillapasa K (2020) Evaluation of optimization parameters of semi-solid metal 6063 aluminum alloy from friction stir welding process using factorial design analysis. J Manuf Mater Proc 4(4):123. https://doi.org/10.3390/jmmp4040123.

[20] Rakesh Roshan, Ajit Kumar Naik, Kuldeep Kumar Saxena, Kanwer Singh Arora, Nikhil Shajan, Velaphi Msomi, Husain Mehdi, Effect of welding speed and wire feed rate on arc characteristics, weld bead and microstructure in standard and pulsed gas metal arc welding, Journal of Adhesion Science and Technology, 2023. https://doi.org/10.1080/01694243.2023.2192314.

[21] Abd Elnabi, M.M., El Mokadem, A. & Osman, T. Optimization of process parameters for friction stir welding of dissimilar aluminum alloys using different Taguchi arrays. Int J Adv Manuf Technol 121, 3935–3964 (2022). https://doi.org/10.1007/s00170-022-09531-3.

[22] Husain Mehdi, Sipokazi Mabuwa, Velaphi Msomi, Kuldeep kumar Yadav, Influence of Friction Stir Processing on the Mechanical and Microstructure Characterization of Single and Double V-Groove Tungsten Inert Gas Welded Dissimilar Aluminum Joints. Journal of Materials Engineering and Performance (2022). https://doi.org/10.1007/s11665-022-07659-7.

[23] Haribalaji V, Sampath Boopathi M, Asif M (2022) Optimization of friction stir welding process to join dissimilar AA2014 and AA7075 aluminum alloys. Materials Today: Proceedings 50(5):2227–2234. https://doi.org/10.1016/j.matpr.2021.09.499.

[24] Abdul Wahab Hashmi, Husain Mehdi, R. S. Mishra, Prabhujit Mohapatra, Neeraj Kant, Ravi Kumar, Mechanical Properties and Microstructure Evolution of AA6082/Sic Nanocomposite Processed by Multi-Pass FSP. Transactions of the Indian Institute of Metals 2022; 75: 2077–2090. https://doi.org/10.1007/s12666-022-02582-w

[25] Benjamin I. Attah, Sunday A. Lawal, Katsina C. Bala, Omolayo M. Ikumapayi, Suryakanta Sahu, Md Iqbal Perwej, Esther T. Akinlabi, Effects of material placement and speed of tool rotation on the tensile strength of dissimilar friction stir welded AA7075-T651 and AA1200-H19 aluminium alloys, materialstoday proceedings, 62 (6), 2022, 4275-4282.

[26] Husain Mehdi, Sumit Jain, Msomi, V. et al. Effect of Intermetallic Compounds on Mechanical and Microstructural Properties of Dissimilar Alloys Al-7Si/AZ91D. J. of Materi Eng and Perform (2023). https://doi.org/10.1007/s11665-023-08302-9.

[27] Sumit Jain, R.S. Mishra, Husain Mehdi, H. Influence of SiC Microparticles and Multi-Pass FSW on Weld Quality of the AA6082 and AA5083 Dissimilar Joints. Silicon (2023). https://doi.org/10.1007/s12633-023-02455-x.

[28] Y.J. Kwon, I. Shigematsu, N. Saito, Dissimilar friction stir welding between magnesium and aluminum alloys, Materials Letters 62 (2008) 3827–3829.

[29] Husain Mehdi, R.S. Mishra, Modification of Microstructure and Mechanical Properties of AA6082/ZrB2 Processed by Multipass Friction Stir Processing. J. of Materi Eng and Perform 32, 285–295 (2023). https://doi.org/10.1007/s11665-022-07080-0

[30] Barooni, O., Abbasi, M., Givi, M. et al. New method to improve the microstructure and mechanical properties of joint obtained using FSW. Int J Adv Manuf Technol 93, 4371–4378 (2017). https://doi.org/10.1007/s00170-017-0810-3.

[31] B. Abnar, M. Kazeminezhad, A.H. Kokabi, Effects of heat input in friction stir welding on microstructure and mechanical properties of AA3003-H18 plates Author links open overlay panel, Transactions of Nonferrous Metals Society of China, 25 (7), 2015, 2147-2155.

[32] Husain Mehdi, R.S. Mishra, Investigation of mechanical properties and heat transfer of welded joint of AA6061 and AA7075 using TIG+FSP welding approach, Journal of Advanced Joining Processes, 1, 2020, 100003.

[33] Schmidt H, Hattel J, Wert J. An analytical model for the heat generation in friction stir welding [J]. Modelling and Simulation in Materials Science and Engineering, 2004, 12: 143157.
[34] Husain Mehdi, R.S. Mishra, Effect of friction stir processing on mechanical properties and heat transfer of TIG welded joint of AA6061 and AA7075, Defence Technology, 17(3), 2021, 715-727.
[35] Kumar R, Singh K, Pandey S. Process forces and heat input as function of process parameters in AA5083 friction stir welds [J]. Transactions of Nonferrous Metals Society of China, 2012, 22(2): 288298.
[36] Sipokazi Mabuwa, Velaphi Msomi, Husain Mehdi, Kuldeep Kumar Saxena, Effect of material positioning on Si-rich TIG welded joints of AA6082 and AA8011 by friction stir processing, Journal of Adhesion Science and Technology, 37(17), 2484-2502, 2022. https://doi.org/10.1080/01694243.2022.2142366.

***Cite this article as*:** Prem Kumar, Kalyan Singh, Azazullah, Optimization of FSW parameters on mechanical properties of AA6082 and AA7475 by response surface methodology, International Journal of Research in Engineering and Innovation Vol-8, Issue-1 (2024), 30-40. *https://doi.org/10.36037/IJREI.2024.8105*.